**Bessam AMROUCHE [1], Haroune AOUZELLAG[1], Koussaila IFFOUZAR [2], Sabrina NACEF [1], Tahar Otmane CHERIF [3] ,Kaci GHEDAMSI[1]**

Laboratoire de Maitrise des Energies Renouvelables, Faculté de Technologie, Université de Bejaia, Algiers (1)
Laboratoire des Sciences Appliquées, Ecole Nationale Supérieure des Technologies Avancées ENSTA d'alger, Algiers (2)
Laboratoire de Conception et Conduite des Systèmes de Production, Faculté de Génie Electrique et Informatique, Université de Tizi Ouzou, 15000, Algeria (3)

doi:10.15199/48.2024.03.20

# Power management for HEV based on PMSM using passivity control

***Abstract.*** *This article offers a resolution of a problem of coordination of the converters of a system fuel cell involving a hydrogen fuel cell with super capacitors as an application with an instantaneous dynamic power by using a non-linear controller PI. The strategy of management of energy include the strategy of control of the state machine, the strategy of proportional control - classical integral (CPICS), and the proof of the stability of the whole source system in a continuous loop closed have were shown simulation and results on a system has reduced ladder prove the feasibility of proposed for a true system transports electrical.The total model of system and the strategy of control is produced by using Matlab / Simulink*

***streszczenie:*** *W artykule zaproponowano rozwiązanie problemu koordynacji przetwornic układu ogniw paliwowych z udziałem wodorowego ogniwa paliwowego z superkondensatorami jako aplikacji o chwilowej mocy dynamicznej z wykorzystaniem nieliniowego regulatora PI. Strategia zarządzania energią obejmująca strategię sterowania maszyną stanów, strategię sterowania proporcjonalnego - całka klasyczna (CPICS) oraz dowód stabilności całego systemu źródłowego w ciągłej pętli zamkniętej przedstawiono symulację i wyniki na systemie o zredukowanej drabinie udowodniono wykonalność proponowanego dla rzeczywistego systemu transportów elektrycznych. Całkowity model systemu i strategia sterowania jest tworzony z wykorzystaniem Matlaba/Simulinka. (**Zarządzanie energią dla HEV w oparciu o PMSM z wykorzystaniem kontroli pasywności**)*

**Keywords:** Fuel-cell, super capacitors, hybrid electric vehicle, energy management strategie.
**Słowa kluczowe:** ogniwo paliwowe, superkondensatory, hybrydowy pojazd elektryczny, strategia zarządzania energią.

Air pollution caused mainly by conventional combustion vehicle classified as classical car and the employment of battery as the only source of energy for electric vehicles (first proposed solution) is still restricted because of its low autonomy, lifetime and charging time problems [1]. In support, the FC is as a good alternative source to its high autonomy and its zero emission of polluting gas [2, 3]. Between the different FC technologies, the Proton Exchange Membrane (PEMFC) is very useful for the transportation area [4, 5]. PEMFC offers a lot of benefits such as the working at a low temperature compared to other types of FC, low cost which is very important point, quick start up and high efficiency. Just, the FC cannot respond to fast transient peak power demand [6, 7] The vehicle speed and power fluctuations may lead to pressure oscillation and oxygen starvation in the FC membrane which can affect the cell life-time[3, 8]. To solve this problem, a hybridization with another source as UC is the most excellent solution to assist the FC source [9]. This system was used not only to cover the peak power demand, but also to recover the braking energy. Therefore, such configuration improved efficiency and satisfied the power drive demands in all driving conditions. The problem of the use of more than one energy source is the power management. In the literature, different strategies have been emerged to solve this problem. This strategies include the state machine control in tramway [10], which is a simple and well-known rule based strategy; each state is given after on heuristic or empiric past experience. In [11], the FC supplied power to UC source to maintain them charged. Recently, energy management based on classical PI controllers has been proposed and the experience is not necessary, and the PI controller can be easily tuned by an optimization algorithm for better tracking. This strategy is based on the control of the main performance parameters, such as the UC state of charge (SOC). Another power management strategy and structure of HEV enveloping operation modes using a battery as secondary source depending on the power demand and the SOC of the battery was developed in [12], the use of the battery as a second source return to same problem cited before and it does not support abrupt power variations. Also, an others type of control strategies and HEV structures were regrouped by authors of [4] to reduce the hydrogen consumption. Others used a fuzzy logic control to supervise.

The power exchange between the FC and the second source in FC/UC and FC/Battery HEV. This control was presented in [13], cascaded with wavelet strategy in [14] and combined with the flatness control technique in [15]. A several fuzzy supervisor developed by authors of [16] to an online controller in order to reduce power losses.

This work considers a parallel architecture that hybridises a fuel cell (FC) as the primary source and an FC module as the secondary source with two static converters. This strategy is based on frequency domain decoupling of the characteristics of each source and uses DC bus control. Finally, a MATLAB simulation is performed and the simulation results are analyzed in more detail.

The HEV is propelled by Permanent Magnet Synchronous Motor (PMSM) connected to the wheels. The global scheme of the HEV and power system of the FC/Ucis represented in Fig. 1 [5]. The two energy sources (FC and UC) exchange power with a DC bus. For the FC, a boost converter unidirectional in current is utilized to connect the FC to the DC bus; although, the UC requires DC/DC converter bidirectional in current to supply power and to recover the breaking energy. The two inductances added as filters and to respect sources alternation. The DC bus which is a capacitor supplies the both traction machines with employing a tow levels inverter to convert the DC power into AC power. This system gives the torque control of wheels in dependently with a significantly high accuracy, which can enhance the stability of the HEV, reduce clutter caused by the mechanical part such as electrical differential and transmission shafts and give more frees space in the vehicle for UC and hydrogen tank. In an electric vehicle (EV) or hybrid electric vehicle (HEV), the PMSM is typically connected to the vehicle's wheels and is controlled by sophisticated power electronics and control systems. These

systems manage the speed, torque, and energy flow between the motor, the vehicle's energy storage system (such as batteries or ultracapacitors), and the driving conditions. The paper is divided into four main parts; the first part is the modelling of the different elements of the system. The second part will deal with the control of the hybrid vehicle. The third part will deal with the control of each element of the system using passivity-based control IDA-PBC for the two sources [5] and FOC for the PMSM [17]. This work will be concluded with the interpretation of the results and the resulting conclusion

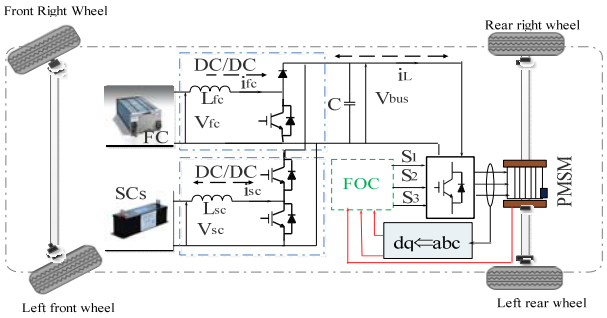


Fig. 1. Global system scheme

## 2. System modeling

For the FC, a boost converter unidirectional in current is utilized to connect the FC to the DC bus; although, the UC requires DC converter bi-directional in current to supply power and to recover the breaking energy. The two inductances ($L_{fc}$ and $L_{sc}$) added as filters and to respect sources alternation. The DC bus which is a capacitor ($C_{bus}$) supplies the traction machine with employing a three phase inverter to convert the DC power into AC power. The machine is three-phase permanent magnet synchronous machine type which is recently used in the transportation field due to its good power, high efficiency The PEMFC is the main energy source for the vehicle. Its cell voltage and its total power are defined by the following equations [4,18]

### 2.1. PEMFC dynamic model

(1) $$V_{\mathrm{fc}} = N_0 V_{\mathrm{fc,cell}}$$

(2) $$V_{\mathrm{fc,cell}} = E + U_{\mathrm{act}} + U_{\mathrm{ohm}}$$

(3) $$U_{ohm} = -R_{\mathrm{fc}}\, i_{\mathrm{fc}}$$

(4) $$U_{\mathrm{act}} = -\frac{B}{N_0}\ln\left(Ci_{\mathrm{fc}}\right)$$

The expression of the Nernst equation according to JC Pamphlet is given by:

(5) $$E_{\mathrm{Nernst}} = E_0 + \frac{RT_{\mathrm{fc}}}{2\mathrm{F}}\ln\left(\frac{P_{\mathrm{H_2}}\sqrt{P_{O2}}}{P_{H2O}}\right)$$

The FC should be able to provide the power demand of the vehicle $P_{dem}$ by taking into account the FC efficiency $\eta_{fc}$

(6) $$\frac{q_{\mathrm{H_2}}}{P_{\mathrm{H_2}}} = K_{\mathrm{H_2}}$$

(7) $$\frac{q_{\mathrm{O_2}}}{P_{\mathrm{O_2}}} = K_{\mathrm{O_2}}$$

(8) $$\frac{q_{\mathrm{H_2O}}}{P_{\mathrm{H_2O}}} = K_{\mathrm{H_2O}}$$

where $K_{H_2}$ and $K_{O_2}$ are the hydrogen and oxygen valve constants respectively.

Using the ideal gas formula and writing the molar flows as $q^{in}$, $q^{out}$ and $q^{r}$, the partial pressures derivation is expressed as:

(9) $$d/dtP_{(H_2)} = (RT_f c)/V_a n(q^i_{(H_2)} n - q^o_{(H_2)} ut - q^r_{(H_2)})$$

(10) $$\frac{d}{dt}P_{\mathrm{O_2}} = \frac{RT_{\mathrm{fc}}}{V_{\mathrm{an}}}\left(q^{in}_{\mathrm{O_2}} - q^{out}_{\mathrm{O_2}} - q^{r}_{\mathrm{O_2}}\right)$$

(11) $$d/dtP_{(H_2O)} = (RT_f c)/V_a n(-q^o_{(H_2O)} ut + q^r_{(H_2O)})$$

As the electromechanical fundamentals are taken in consideration, the molar flows of the both gas can be written as:

(12) $$q^r_{(H_2)} = N_0/2FI_f c = 2K_r I_f c$$

(13) $$q^r_{\mathrm{O_2}} = \frac{N_0}{4F} I_{\mathrm{fc}} = K_{\mathrm{r}} I_{\mathrm{fc}}$$

(14) $$q^r_{\mathrm{H_2O}} = \frac{N_0}{2F} I_{\mathrm{fc}} = 2K_{\mathrm{r}} I_{\mathrm{fc}}$$

where:

(15) $$\frac{d}{dt}P_{\mathrm{H_2}} = \frac{RT_{\mathrm{fc}}}{V_{\mathrm{an}}}\left(q^{in}_{\mathrm{H_2}} - K_{\mathrm{H_2}}P_{\mathrm{H_2}} - 2K_{\mathrm{r}}I_{\mathrm{fc}}\right)$$

(16) $$\frac{d}{dt}P_{\mathrm{O_2}} = \frac{RT_{\mathrm{fc}}}{V_{\mathrm{an}}}\left(q^{in}_{\mathrm{O_2}} - K_{\mathrm{O_2}}P_{\mathrm{O_2}} - K_{\mathrm{r}}I_{\mathrm{fc}}\right)$$

(17) $$\frac{d}{dt}P_{\mathrm{H_2O}} = \frac{RT_{\mathrm{fc}}}{V_{\mathrm{an}}}\left(K_{\mathrm{H_2O}}P_{\mathrm{H_2O}} + 2K_{\mathrm{r}}I_{\mathrm{fc}}\right)$$

Assuming that the initial conditions of the hydrogen and oxygen partial pressures are equal to zero, the Laplace transforms of (16), (17) and (18) are expressed as:

(18) $$\tau_{\mathrm{H_2}} = \frac{V_{\mathrm{an}}}{K_{H_2}RT_{\mathrm{fc}}} \quad \tau_{\mathrm{O_2}} = \frac{V_{\mathrm{an}}}{K_{O_2}RT_{\mathrm{fc}}} \quad \text{and} \quad \tau_{\mathrm{H_2O}} = \frac{V_{\mathrm{an}}}{K_{H_2O}RT_{\mathrm{fc}}}$$

The fuel cell model is shown in the Fig. 2.

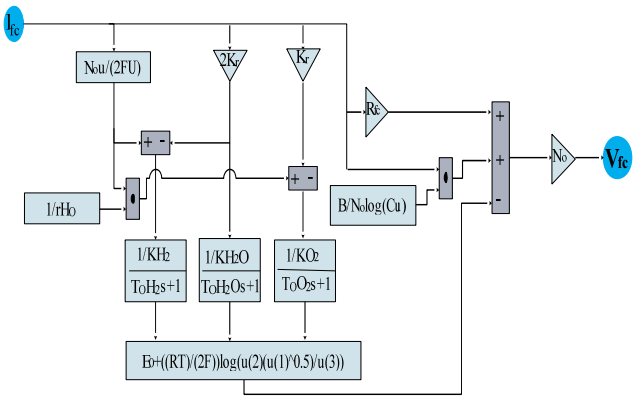


Fig. 2. Mathematical model of the fuel cell

### 2.2. UC system modeling

The UC is chosen as a second energy source because of its considerably high power densities, its unlimited number of charge and discharge cycle compared to the battery and low temperature performance [3]. Moreover, it is robust and maintenance free. EDLC is an electrochemical capacitor that consists of two electrodes to allow a potential to be applied across the cell; two double layers are therefore present, one at each electrode/electrolyte interface.

The dynamic model represents the electrochemical behavior of UC. In this paper, a mathematical model consisting of Stern and Tafel equations is used that gives the relationship between voltage, current and the available amount of charge during charging/discharging processes [23]. The input of this model is the current obtained from theterminal of EDLC, and the outputs are the voltage and the *SOC* of UC. The detailed block diagram of the dynamic model is illustrated in Fig. 3.

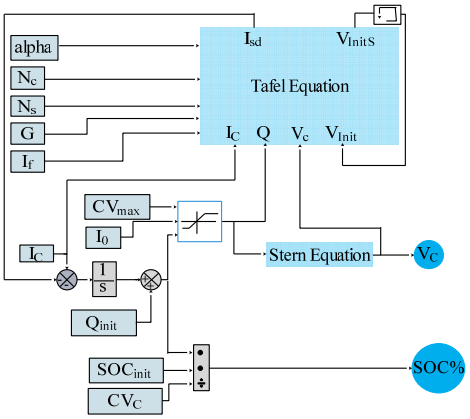


Fig. 3. Block diagram of the detailed dynamic model.

The amount of electric charge in $U_C(Q)$ is calculated as in (20), where $Q_{init}$ is the initial amount of charge, $I_c$ is the measured current, and $i_{sd}$ is the self-discharge current:

$$(19)\quad Q = Q_{\text{int}} + \int_0^t -\left(i_{\text{c}}(\tau) + i_{\text{sd}}(\tau)\right) d\tau$$

he saturation limit function is used to restrict the calculated amount of charge within a specific range to prevent the full discharge and overcharge of UC. The Tafel equation given in (21) is used to calculate the leakage current $i_{sd}$ that represents the self-discharge phenomenon of UC:

$$(20)\quad -i_{\text{sd}}(t) = A i_0 N_{\text{c}} e^{\left(\frac{\alpha}{R}\frac{F}{T_{\text{c}}}\left(\frac{V_{\text{c}}}{N_{\text{S}}} - \frac{V_{\text{c,max}}}{N_{\text{S}}} - \Delta V_{\text{c}}\right)\right)}$$

$$(21)\quad V_c = \frac{N_{\text{c}} N_{\text{s}} Q x_2}{N_{\text{p}} N_{\text{c}}^2 \varepsilon \varepsilon_0 A} + \frac{N_{\text{c}} N_{\text{s}} 2RT_{\text{c}}}{F} \operatorname{arsinh}\left(\frac{Q}{N_{\text{p}} N_{\text{c}}^2 A\sqrt{8RT_{\text{c}}\varepsilon\varepsilon_0 c}}\right)$$

The SOC for a fully charged UC is $100\%$ and for an empty UC is $0\%$. The SOC is calculated as:

$$(22)\quad SOC = \frac{Q_{\text{init}} - \int_0^t i_{\text{c}}(\tau) d\tau}{Q_{\text{max}}} 100$$

### 2.3 Three-Phase PMSM Modeling

The electrical equations of three-phase PMSM in $q$ and $d$ frame can be expressed :

$$(23)\quad \begin{cases} \text{v}_d = R_d i_d + \dfrac{d}{dt}\varphi_d - \omega\varphi_q \\ \text{v}_q = R_q i_q + \dfrac{d}{dt}\varphi_q + \omega\varphi_d \end{cases}$$

$$(24)\quad \begin{cases} \dfrac{d}{dt} i_d = \dfrac{1}{L_d}\left(V_d - R i_d + L_q \omega i_q\right) \\ \dfrac{d}{dt} i_q = \dfrac{1}{L_q}\left(V_q - R i_q - L_d \omega i_d - \varphi_f \omega\right) \end{cases}$$

The electromagnetic torque can be expressed as:

$$(25)\quad T_{em} = p\left(\left(L_d - L_q\right) i_d i_q + \varphi_f i_q\right)$$

Where $p$ the PMSM poles number.
The torque and rotor speed are given as follow:

$$(26)\quad \frac{d}{dt}\Omega = \frac{1}{J}\left(T_{em} - f\,\Omega - T_r\right)$$

Where $J$, $\Omega$, , $T_r$ and $f$ total inertia brought back to the rotor, rotor mechanical speed, load torque and friction coefficient of motor respectively.
where $\Omega = p\,\omega$ and $\omega$: electrical pulsation
The power absorbed by the PMSM is given by the following equation:

$$(27)\quad P_a = {2\pi n_s T}/{60}$$

where $n_s$ is The speed of the rotating field in (rpm)

### 2.4. Vehicle modeling

The vehicle is considered as a solid point moving subjected to forces along the longitudinal axis: the traction forces $F_t$ caused by the action of the two drive wheels, the friction force to the advancement $F_{roll}$ , the effort of aerodynamic resistance $F_{\text{aero}}$ and the resistance of mounted side $F_{slope}$ [19,20]. The resisting forces are given by the following equations:

$$(28)\quad F_{\text{roll}} = M_{\text{v}}\, g\, f_{\text{r}}$$

$$(29)\quad F_{\text{aero}} = \frac{1}{2}\rho A C_{\text{x}} V_{\text{v}}^2$$

$$(30)\quad F_{\text{slope}} = M_{\text{v}}\, g \sin(\delta)$$

The fundamental principle of the vehicle dynamics is described by the following equation:

$$(31)\quad M_{\text{v}}\frac{dV_{\text{v}}}{dt} = F_{\text{t}} - F_{\text{roll}} - F_{\text{aero}} - F_{\text{slope}}$$

The traction force of each wheel is given by the following expression:

$$(32)\quad \frac{F_{\text{t}}}{2} = \frac{T}{2R_{\text{w}}}$$

### 2.5 SCs boost converter

in this paper SCs are used for two types of operations, the mode of working when SCs receives the uninterrupted energies of the bus of current and the second mode when SCs gives the energies in the bus of current go on, therefore the storage elements are connected to the DC bus through a reversible power converter, The boost converter is controlled by binary input. We define $\lambda_2$ as the duty cycle of the control variable. The second sub-system is represented by an average model as follows:

$$(33)\quad \frac{d}{dt}(i_{sc}) = \frac{1}{L_{SC}}\left(-\left(1-\lambda_2(t)\right)v_b(t) + v_{sc}(t)\right)$$

$$(34)\quad \frac{d}{dt}v_{sc}(t) = -\frac{i_{sc}(t)}{C_{sc}}$$

where $v_{sc}(t)$ is the SCs voltage, $v_b$ is the DC link voltage, $i_{sc}$ is the SCs current, $L_{SC}$ is the inductance of the SCs and $C_{sc}$ is the capacity of the SCs

### 2.6 FC boost converter

A lifting converter must augment voltage $v_{fc}$, by what voltage, $v_{fc}$ is often less than the voltage of bus of direct current, is controlled by binary input. Defining $\lambda_1$ as the duty cycle of control variable

knowing that the currents $i_{fc}$ and $i_L$ are physically the same . The dynamics of the DC–DC boost power converter with an inductive load This sub-system is represented by an average model as follows :

$$\frac{d}{dt}i_{fc}=\frac{1}{L_{fc}}\left(-\left(1-\lambda_1(t)\right)v_b(t)+v_{fc}(t)\right) \quad (35)$$

$$\frac{d}{dt}v_b(t)=\frac{1}{C_b}\left(\left(1-\lambda_1(t)\right)i_{fc}(t)+\left(1-\lambda_2(t)\right)i_{sc}(t)-i_L(t)\right) \quad (36)$$

where $v_{fc}$ is the FC voltage, $i_L$ is the DC current delivred to the load and $i_{fc}$ is the FC current

In our work, the load is modeled by a Permanent magnet synchronous machine; the model is represented in the reference mark(d ,q).

$$\frac{d}{dt}i_L(t)=\frac{1}{L}\left(-R_l(t)i_L+v_b(t)-\varphi_f\omega(t)\right) \quad (37)$$

$$\frac{d}{dt}\Omega=\frac{1}{J}\left(p\left(\left(L_d-L_q\right)i_d i_q+\varphi_f i_q\right)-f\,\Omega-T_r\right) \quad (38)$$

**Complete model**. It follows that the complete "fuel cell - super capacitors" system is represented by the 5th order non-linear state space model :

$$\begin{cases}\frac{d}{dt}v_b(t)=\frac{1}{C_b}\left(\left(1-\lambda_1(t)\right)i_{fc}(t)+\left(1-\lambda_2(t)\right)i_{sc}(t)-i_L(t)\right)\\ \frac{d}{dt}v_{sc}(t)=-\frac{i_{sc}(t)}{C_{sc}}\\ \frac{d}{dt}i_L(t)=\frac{1}{L}\left(-R_l(t)i_L+v_b(t)-\varphi_f\omega(t)\right)\\ \frac{d}{dt}i_{fc}=\frac{1}{L_{fc}}\left(-\left(1-\lambda_1(t)\right)v_b(t)+v_{fc}(t)\right)\\ \frac{d}{dt}(i_{sc})=\frac{1}{L_{SC}}\left(-\left(1-\lambda_2(t)\right)v_b(t)+v_{sc}(t)\right)\end{cases} \quad (39)$$

with state space $x(t)=\left[v_b;v_{sc};i_L;i_{fc};i_{sc}\right]^T$ ,control imputs $u(t)=\left[u_1;u_2\right]^T=\left[1-\lambda_1;1-\lambda_2\right]^T$ ,measures $y(T)=x$ and $v_{fc}$.

the system equation (39) is called an unsettled system since the difference of ladder of time between the dynamics of voltages and the current them causes it of disturbance, to resolve this problem the system in mode controlled is forced by current by using a loop inner current. More precisely, the following PI current controllers.

$$u_1=Ki_{fc}\int_0^t\left(i_{fc}^*-i_{fc}\right)dt+Kp_{fc}\left(i_{fc}^*-i_{fc}\right) \quad (40)$$

$$u_2=Ki_{sc}\int_0^t\left(i_{sc}^*-i_{sc}\right)dt+Kp_{sc}\left(i_{sc}^*-i_{sc}\right) \quad (41)$$

In equations 40 and 41, $u_1$ and $u_2$ have been programmed to individually compel the $i_{fc}$ and $i_{sc}$ currents to obey their references $i_{fc}^*$ and $i_{sc}$ , resulting in an extremely rapid response time when the static error occurs. The two control laws $u_1$ and $u_2$ function as high gain feedback, the two static gains are deemed suitably strong in terms of the voltage and load dynamics, and after the transient we obtain $i_{fc}{}^*-i_{fc}=0$ and $\int_0^t\left(i_{fc}^*-i_{fc}\right)=v_{fc}/v_b\,Ki_{fc}$ , this means that the equation 40 becomes $u_1=v_{fc}/v_b$ and according to the same argument the equation 41 becomes $u_2=v_{sc}/v_b$ . therefore by replacing the two new control laws and current $i_{fc}^*$ and $i_{sc}^*$ them in the global system we obtain the following reduced order system [21]

$$\begin{cases}\frac{d}{dt}v_b(t)=\frac{1}{C_b}\left(\frac{v_{fc}(t)}{v_b(t)}i_{fc}{}^*(t)+\frac{v_{sc}(t)}{v_b(t)}i_{sc}{}^*(t)-i_L(t)\right)\\ \frac{d}{dt}v_{sc}(t)=-\frac{i_{sc}{}^*(t)}{C_{sc}}\\ \frac{d}{dt}i_L(t)=\frac{1}{L}\left(-R_L(t)i_L+v_b(t)-E(t)\right)\end{cases} \quad (42)$$

according to the control by passivity and the Hamiltonian modeling the resolution of the equations of states representing the static converters [21,6] we will obtain the referential equations of the currents as

$$\begin{cases}\boldsymbol{i_{fc}}^*=\frac{v_{bus}}{v_{fc}}\left[i_L{}^*+\lambda\left(\left(\frac{v_{sc}}{v_{bus}}-\frac{v_{bus}}{v_{fc}}\right)\tilde{v}_{bus}-\tilde{v}_{sc}\right)\right]\\ \boldsymbol{i_{sc}}^*=-\lambda\tilde{v}_{bus}\end{cases} \quad (43)$$

## 3. Control system

### 3.1 Field oriented control of PMSM

The aim is always to assimilate the behavior of PMSM to that to the DC machine separately excited by decoupling control of torque of the flux. The model exprimed in system (23) is strongly coupled, which make it very difficult to resolve. For this the decoupling of this later is most interesting

The model of the synchronous machine in the reference rotational frame (dq) to system differential equations where the currents $i_d$ and $i_q$, are not independent one of the other. They are connected by nonlinear terms $L_q\omega i_q$ and $L_d\omega i_d$

$$\begin{cases}V_d=\left(Ri_d+L_d\frac{d}{dt}i_d\right)-L_q\omega i_q\\ V_q=\left(Ri_q+L_q\frac{d}{dt}i_q\right)+L_d\omega i_d+\varphi_f\omega\end{cases} \quad 42)$$

then the method of the compensation is useful has the elimination of this coupling, this last method consists has to add terms to the levels of the two axes in order to return them independent completions. The principle of this decoupling return has to define two new variables $e_d$ and $e_q$ of orders as follows such as

$$\begin{cases}V_d=V_{d1}-e_d\\ V_q=V_{q1}+e_q\end{cases} \quad (43)$$

with

$$\left\{V_{d1}=Ri_d+L_d\frac{d}{dt}i_d \quad Ri_q+L_q\frac{d}{dt}i_q\right. \quad (44)$$

and

$$(45)\begin{cases} e_d = L_q \omega i_q \\ e_q = L_d \omega i_d + \varphi_f \omega \end{cases}$$

finally we will have both of this month who are uncoupled

$$(46)\begin{cases} i_d = \dfrac{V_{d1}}{R_s + pL_d} \\ i_q = \dfrac{V_{q1}}{R_s + pL_q} \end{cases}$$

$p$: Operator of Laplace.

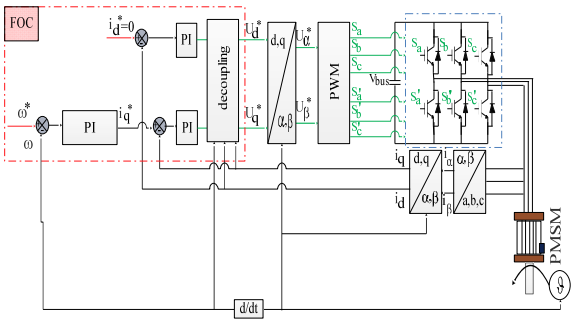


Fig. 4. Block diagram of field oriented control (FOC)

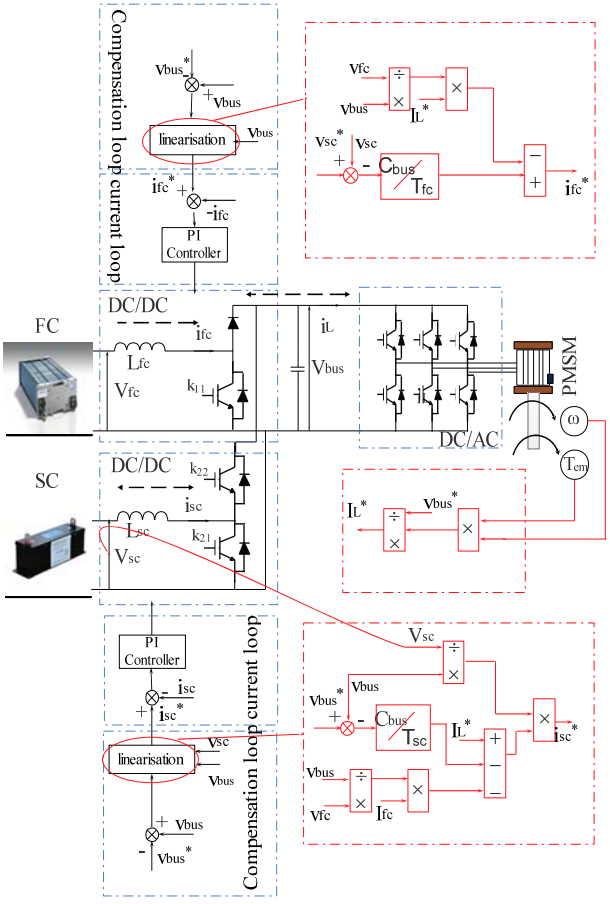


Fig. 5. Bloc diagram of the control strategy

### 3.2 Power management strategies

The control of the two converters system has been detailed in [21] It consists on the frequency decoupling of sources according to the power requested. The DC bus filters the high frequencies, the SCs connected with its converter provides the medium frequencies and the FC ensures the low frequencies. This frequency decoupling of the sources naturally induces a power management strategy based on cascaded loops presented in Fig. 5.

Any change in the DC bus voltage is induced by power load modification. Hence, it seems recommended to control the DC bus voltage with the SCs by computing the reference current $i_{sc}$, and thus regulate the bus voltage to its reference. The outer voltage loop associated with the SCs management must maintain the DC bus voltage at a constant reference $v_{bus}$ fixed at $400V$. The current loops are based on proportional-integral controller.

Knowing that the demand for DC bus assistance would result in a permanent SC discharge, which would impose an excessive capacity to provide and continuously absorb energy during rapid transient regimes. Therefore, the control system must maintain, in steady state, the SC state of charge at a desired value and avoid huge SCs voltage ripple. This requirement can be ensured by a compensation loop whose purpose is to regulate the SCs voltage $v_{sc}$ at their references $v_{sc}^*$.

The compensation is assured by a proportional integral regulator. Thus the compensation loop generates a current reference $i_{fc}^*$ with a slow dynamic. Consequently, this choice meets the frequency decoupling requirement and allows good control of the SCs to their voltage reference levels.

### 5 simulations and results

The analysis will focus on the Transitional FC / SC System Fig.6 shows the response of the hybrid system for both architectures to a load including positive and negative current steps (Fig.6. (a),(c),(i)). At each transient load (T = 0.1 s / 2.5 s / 6 s), the bus voltage for the two-converter structure (Figure.6 (e), (f)) is slightly transiently affected (less than 4%) but is generally well regulated. We observe a slow variation of the FC voltage, but it nevertheless remains subject to its reference. Indeed, this is made possible by the super capacitors that react

Rapidly to the sudden transients of the charging current (Fig. 6 (e)). These transients are induced by the regulation of the bus voltage and make it possible to ensure the major part of the transient component of the required power. The energy transfer from the SCs to the DC bus is therefore logical and correct and makes it possible to compensate for the energy that is not supplied by the fuel cell. This allows the cell to respond without abrupt change in its current stress to the load

Then, as the current of the FC increases, the discharge Of the SCs characterized by the decrease of its voltage is attenuated until it cancels out (Fig. 6 (b)). There is then a regime of rebalancing (called compensation), Characterized by a recharge of the SCs at its values of Reference ($V_{scref}$) set at 100V.

During the negative current transients of the load (at times t = 2.5 s / 6s), the load is fed by the FC but part of the excess power of this load is absorbed by the SCs (HF) .Subsequently, rebalancing (compensation) takes place because the FC progressively supplies the power required for the load, as well as that necessary to bring the voltages of the SCs back to their reference levels. In this case, it may be a power lower than that required by the load so that the voltage of the SCs decreases towards its reference level.

The recuperative functioning is envisaged in the simulation. However, the sudden drop in load power creates recuperative operation at the SCs

The following figure shows the result of the vector control of PMSM using the proportional integral action. The nominal load of $250\ N.m$ (Fig. 6 (h)) is proportional to the speed of the vehicle and the distance traveled. The result of the simulation shows the behavior of the PMSM with vicotrial

control. The mechanical speed and the electromagnetic torque follow perfectly the reference (Fig. 6 (g), (h)). Thus, the quadratic current is the image of the

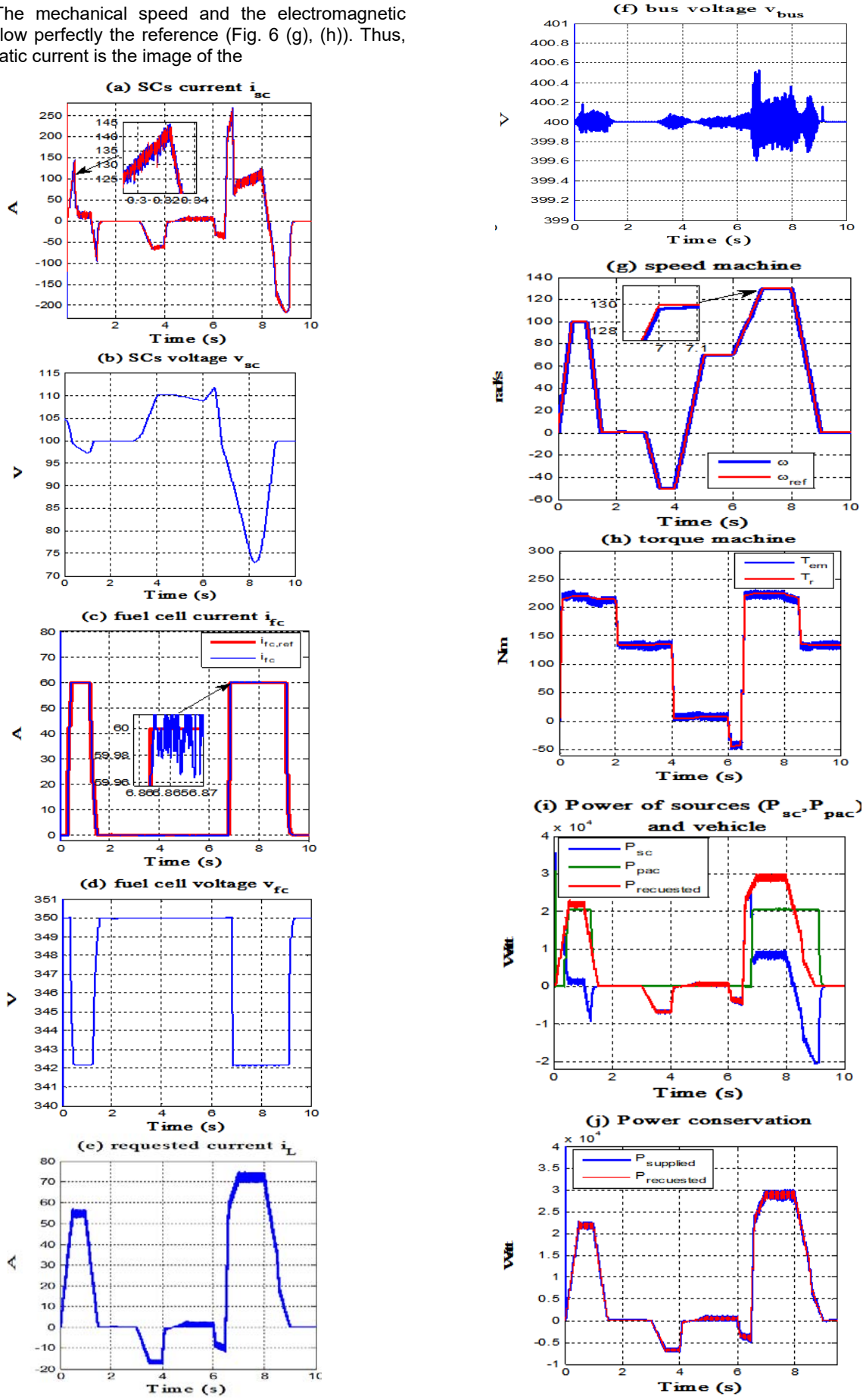


Fig. 6. Simulation system results

## Conclusion

The integration of permanent magnet synchronous machines (PMSMs) in electric vehicles (EVs) is a significant topic in the field of electric vehicle propulsion systems and motor drive technology. PMSMs are a type of electric motor that offers several advantages for EV applications, making them a popular choice for electric propulsion. The passivity-based control method used in this article aims to define controllers that feature system . stability and performance while preventing instability or unpredictable behavior. A control strategy for an electric vehicle is essential to maximize energy efficiency, optimize the management of electrical sources and improve the overall performance of the vehicle

**Appendix A.** Table 1: Electric characteristics of the hybrid system.

| parametre | Value |
|---|---|
| Fuel cell parametre | |
| Open circuit voltage E | $350V$ |
| Rated voltage | $342\,V$ |
| Rated current | $60\,V$ |
| Supercapacitors parametres | |
| Capacitance | $5\,F$ |
| Rated voltage | $100\,V$ |
| Rated current | $250\,A$ |
| Optimal voltage $v_{sc}^{*}$ | $100\,V$ |
| Exchange current density $i_0$ | $0.05\,A.m-2$ |
| Molar concentration $c$ | $1(8\,NA\,r^3)^{-1}$mol.m$^{-3}$ |
| Number of layers of electrodes $N_c$ | 1 |
| Number of parallel UC cells $N_p$ | 1 |
| Number of series UC cells $N_s$ | 18 |
| Molecular radius $r$ | $10^{-9}$C |
| Charge transfer coefficient $\alpha$ | $0.3\,m$ |
| Permittivity of material $\varepsilon$ | $6.0208\,10^{-10}$F.m$-1$ |
| Over potential $\Delta V_c$ | $2.7\,V$ |
| Operating temperature TC | 25 C° |
| Inductance and capacitie parametres | |
| $L_{sc}$ | $200\,\mu H$ |
| $L_{fc}$ | $100\,\mu H$ |
| Rated current $L_{sc}$ | $250\,A$ |
| Rated current $L_{fc}$ | $60\,A$ |
| Capacities $C$ | $1\,mF$ |
| Optimal DC bus voltage $v_{bus}^{*}$ | $400\,V$ |
| Parameters of the HEV model. | |
| Vehicle total mass | $1300\,Kg$ |
| Rolling resistance force constant | $0.01\,s^2/m^2$ |
| Air density | $1\,Kg.m^3$ |
| Frontal surface area of the vehicle | $2.6\,m^2$ |
| Tire radius | $0.32\,m$ |
| Aerodynamic drag coefficient | 0.30 |
| Acceleration due to gravity | $9.8\,m/s^2$ |
| parameters of PMSM | |
| Speed | $150\,rad/s$ |
| Nominal torque | $250\,N.m$ |
| $R_s$ | $0.5\,\Omega$ |
| $L_d = L_q$ | $8.5\,mH$ |
| $\varphi_f$ | $0.1815\,Wb$ |
| $p$ | 4 |
| $J$ | $0.00546\,Kg.m^2$ |
| $f$ | $0.0112\,m^{-1}$ |

***Authors:*** Bessam AMROUCHE [1], Haroune AOUZELLAG[1], Koussaila IFFOUZAR [2], Sabrina NACEF [1], Tahar Otmane CHERIF [3] ,Kaci GHEDAMSI[1] Laboratoire de Maitrise des Energies Renouvelables, Faculté de Technologie, Université de Bejaia, Algiers, *BP 271 Kherrata bejaia 06004 Email:bessam.amrouche@univ-bejaia.dz.*

## REFERENCES

[1] M D. Berliner, D A. Cogswell , M Z. Bazant *, R D. Braatz A Mixed Continuous-Discrete Approach to Fast Charging of Li-ion Batteries While Maximizing Lifetime IFAC-PapersOnLine 2022, Pages 305-310

[2] H. Aouzellag, B. Amrouche, k. iffouzar D. aouzellag. Proposed hysteresis energy management strategy based on storage system efficiency for hybrid electric vehicle Journal of Energy Storage, 2022, 105259

[3] Azib Toufik, Bethoux Olivier, Remy Ghislain, Marchand Claude. Saturation management of a controlled fuel-cell/ultracapacitor hybrid vehicle. IEEE Trans. Veh. Technol. 2011; 60: 4127–4138.

[4] H S Das , M Salem , M A A M Zainuri , A M Dobi , S Li , Md H Ullah . A comprehensive review on power conditioning units and control techniques in fuel cell hybrid systems Energy Reports, 2022, Pages 14236-14258

[5]A A Sinha , Sanjay , M Z Ansari , A K Shukla [c], T Choudhary . Comprehensive review on integration strategies and numerical modeling of fuel cell hybrid system for power & heat production. International Journal of Hydrogen Energy .2023

[6] B Amrouche , T O Cherif, M Ghanes, K Iffouzar, A passivity-based controller for coordination of converters in a fuel cell system used in hybrid electric vehicle propelled by two seven phase induction motor. Int. J. Hydrogen Energy 2017, 26362-26376.

[7] S Sagaria, RC Neto, P Baptista. Assessing the performance of vehicles powered by battery, fuel cell and ultra-capacitor: Application to light-duty vehicles and buses Energy Conversion and Management, 2021, 113767

[8] A Farsi, M A. Rosen Performance analysis of a hybrid aircraft propulsion system using solid oxide fuel cell, lithium ion battery and gas turbine . Applied Energy, 2023, 120280

[9] C Jia , J Zhou , H He , J Li a c, Z Wei , K Li, M Shi . A novel energy management strategy for hybrid electric bus with fuel cell health and battery thermal- and health-constrained awareness . Energy ,2023, 127105

[10] M Iqbal , M Becherif, H S Ramadan, A Badji. Energy source sizing methodology for hybrid fuel cell vehicles based on statistical description of driving cycle. Applied Energy, 2021, 117345

[11] R T Yadlapalli , R R Alla , R Kandipati , A Kotapati. Super capacitors for energy storage: Progress, applications and challenges Journal of Energy Storage Volume 49, May 2022, 104194

[12]M Hua , C Zhang , F Zhang , Z Li , X Yu , H Xu , Q Zhou .Energy management of multi-mode plug-in hybrid electric vehicle using multi-agent deep reinforcement learning Applied Energy, 2023, 121526

[13] B Jin, L Zhang a, QChen a, Z Fu. Energy management strategy of fuzzy logic control for fuel cell truck. Energy Reports 2023, 247-255

[14] R Koubaa , S Bacha , M Smaoui, L krichen. Robust optimization based energy management of a fuel cell/ultra-capacitor hybrid electric vehicle under uncertainty Energy 2020, 117530

[15] I M Abdelqawee, A W Emam, M S ElBages, M A Ebrahim. An improved energy management strategy for fuel cell/battery/supercapacitor system using a novel hybrid jellyfish/particle swarm/BAT optimizers. Journal of Energy Storage, January 2023, 106276

[16] G Ren, H Wang, CChen, J Wang An energy conservation and environmental improvement solution-ultra-capacitor/battery hybrid power source for vehicular applications. Sustainable Energy Technologies and Assessments, April 2021, 100998

[17] K Iffouzar , B Amrouche , T O Cherif, M F Benkhoris, D Aouzellag , K Ghedamsi . Improved direct field oriented control of multiphase induction motor used in hybrid electric vehicle application. Int. J. Hydrogen Energy 2017, Pages 19296-19308

[18] Q Li , H Yang, Y Han a, MLi b, W Chen. A state machine strategy based on droop control for an energy management system of PEMFC-battery-supercapacitor hybrid tramway. In. J . Hydrogen Energy 2016, 16148-16159

[19] D Rezzak a, N Boudjerda. Robust energy management strategy based on non-linear cascade control of fuel cells-super capacitors hybrid power system. In. J Hydrogen Energy 2020, Pages 23254-23274

[20] H Hu, W W Yuan , M Su , K Ou .Optimizing fuel economy and durability of hybrid fuel cell electric vehicles using deep reinforcement learning-based energy management systems. Energy Conversion and Management September 2023, 117288

[21] Hilairet M, Ghanes M, Bethoux O, Tanasa V, Barbot J-P, Normand-Cyrot D. A passivity-based controller for coordination of converters in a fuel cell system. Control Eng Pract 2013;21(8):1097e109. Pergamon.